

SENSITIVITY TO SPECIMEN IMPERFECTIONS OF IOISIPESCU SHEAR FOR COMPOSITE LAMINATES

L. Niklas Melin, Jonas M. Neumeister

Solid Mechanics, KTH - Royal Institute of Technology, SE -100 44 Stockholm, Sweden

Keywords: *Iosipescu Shear Composite Specimen Imperfection Experiment Numerical*

Abstract

The influence of imperfections in specimen geometry is studied for the Iosipescu test. With FE-analyses and experimental verifications, it is found that slight deviations from nominal geometry in the specimen gripping section may cause errors in measured/calculated strain levels by up to 100%, or even more. Unacceptably large errors may occur already for imperfections in the order of 0.01 mm. Most critical is the case when gripping surfaces are tilted towards each other, giving a stubbed conical shape of the cross section. A rhomboidal cross section does not cause as large front-to-back differences but produces uneven, skewed strain profiles. Numerical calculations show the severity of, and sensitivity to, such imperfections for both isotropic materials and orthotropic composites. And experiments with aluminum- and uniaxial carbon fiber composite specimens with controlled geometrical deviations verify, using in-situ strain field monitoring, that the same phenomena occur also in real experiments, and at comparable magnitudes.

1 Introduction and Background

When testing for material properties, it is important to achieve well controlled, well defined and as pure conditions in the test region as possible. This is intricate in isotropic materials and even more so for composites, particularly so for shear properties[1,2]. A basic requirement is, of course, to have uniform stress- and strain distributions in the test region regardless of which material is tested.

For elastic orthotropic materials, near uniformity is ascertained using a modified (rescaled) specimen[3,4]. A notch opening angle 2θ depending on principal Young's moduli according to

$$\tan(\theta) = \frac{\tan(\theta_{iso})}{\sqrt[4]{\lambda}} \quad (1)$$

where

$$\lambda = \frac{E_y}{E_x} \quad (2)$$

gives essentially uniform conditions[3,7] ($2\theta_{iso} = 110^\circ$ is optimal for isotropic materials, see also Fig. 1). Presumably, non-linear material behaviour such as plasticity or other softening mechanisms tend to weaken the effects of initial non-uniformities if premature failure can be avoided.



Fig. 1. Schematic of Iosipescu test with specimen geometry depending on material orthotropy.

Better testing conditions implies higher attainable loads, which, in turn, requires firmer specimen gripping. It also results in an increased sensitivity to undesired loading states and other imperfections which is the topic of the present study

It is often observed in experiments that actual conditions differ quite substantially from nominal ones[5-7]. For instance, strain readings between front and back may differ substantially. Further damage or failure initiation outside the test region may aggravate such effects, as may an uneven onset of material non-linearity. These effects are attributed to parasitic twisting due to e.g. inadequate fixture function[5], and averaged strain readings are

strongly recommended for measuring moduli and constitutive responses in shear.

A superimposed twisting torque definitely will give erroneous states of strain, and undesired motion and rotation of fixture parts should be completely avoided. However, the same phenomena may arise also with perfect fixture function as is shown here.

2 Sensitivity to Imperfect Specimen Geometry

With specimens differing from nominal geometry (ever so slightly), the arising strain states may be vastly different than expected ones. Even for differences within the ASTM specified tolerances[2], such irregularities cause significant variations in resulting fields.

Of primary concern are straight, parallel and/or perpendicular bounding faces in the clamping sections, i.e. where the loads are applied[6]. In ref. [8], three different types of specimen imperfections were investigated numerically for isotropic materials. This was studied for various magnitudes of the imposed imperfections, here denoted d (see also Fig. 2).

Two of the imperfection types gave notable effects on the stress distribution shapes and levels in the test region (the third primarily affected stresses in the clamping region). The two more crucial imperfections both had gripping surfaces slightly bevelled from the panel surface, i.e. not quite perpendicular to specimen front and back faces. In Fig. 2, the imperfection types identified in ref. [8] are shown, and how their magnitude is defined.

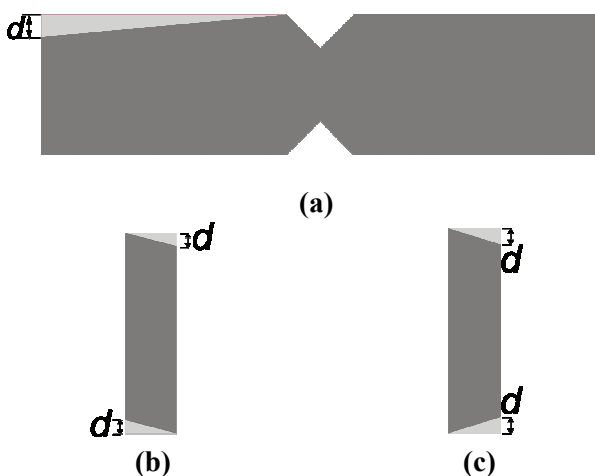


Fig. 2. Three different types of specimen geometrical imperfections[8]: a) non-parallel gripping surfaces (type 1), b) rhomboidal cross section (type 2), and c) conical cross section (type 3). Imperfection magnitude is d .

The non-perpendicular angles of the specimen cross section in its gripping part lead to uneven and non-centered application of the loads due to gripping load and nominal shear. The gripping loads may disturb stress fields also in the test region, but will not affect the shear component of interest, τ_{12} , since clamping is (or should be) symmetrical. The nominal shear load, however, is applied in an anti-symmetrical manner (with respect to the specimen length) cf. Fig. 1a. Thus, the beveled edges will additionally cause non symmetric τ_{12} -profiles also with respect to the (center of the) test region cross section, see Figs. 2bc. These two imperfections will henceforth, based on the shape of their cross section, be referred to as rhomboidal (type-2) and the conical (type-3).

Such imperfections may readily occur when machining specimens, they may arise from worn machining tools, from tool- and/or specimen holder deformation, they may be intrinsic to the machining method and also depend on specimen material. Many high performance composites are very difficult to machine precisely, and usually require very high tool speed and low tool feed. Just a little too hasty machining or insufficient cooling may cause several of the above problems at the same time. Further, such composite laminates are rarely geometrically perfect and planar plates so that even perfect machining does not ensure perfect testing conditions.

In this work, the effects of imperfect specimen geometry are investigated further; Numerically, also anisotropic materials are studied, and moreover the two most crucial imperfections are studied experimentally on especially prepared imperfect specimens using a digital speckle photography (DSP-) technique, which records two-sided full field in-situ strains and displacements

3 FE-modeling of Imperfect Specimens

The imperfect specimens were modeled and evaluated using the commercial FEM package ABAQUS, version 6.6. In the simulations, a specimen was clamped between four discrete rigid planes simulating the fixture. Loads and boundary conditions were applied on these planes (see Fig. 3). Contact was defined between the specimen and these planes.

In the normal direction, 'hard' contact was used and separation was suppressed or allowed depending on if this was expected or not. In the tangential direction, a penalty formulation was used

with friction parameter, $\mu = 0.4$, to control sliding. All the specimens were of thickness 5 mm, height 20 mm and length 80 mm and the length of the test region between the notches was 12 mm.

Although generating very high local stresses, only a linear elastic material model was used for both materials in the models since the main conclusions here do not depend on the local conditions near singularities or contact surfaces.

The isotropic material used is aluminium (Al), and for the composite material, a carbon fiber reinforced epoxy (CFRP-) panel, an orthotropic material model was chosen. The elastic properties for both materials are shown in Table 1.

Table 1 Elastic properties for tested materials.

Material	Young's moduli [GPa]	Poisson's ratios [-]
Al	70	0.3
CFRP	$E_1=140$ $E_2=10$ $E_3=10$	$\nu_{12}=0.30, \nu_{21}=0.02$ $\nu_{13}=0.30, \nu_{31}=0.02$ $\nu_{23}=0.50, \nu_{32}=0.50$

The ratio between clamping and net shear load was studied in refs. [6, 7], and an appropriate value for the clamping ratio P_{clamp}/P_{shear} was found to be about unity. Thus, $P_{clamp} = 4\text{kN}$ and $P_{shear} = 4\text{kN}$, were chosen for specimens of both materials. Loads were applied in the following sequence: first the specimen was clamped and thereafter the net shear load was applied.

In Fig. 3, the FE-model for a rhomboidal specimen imperfection is shown together with all the loads applied and clamping planes indicated.

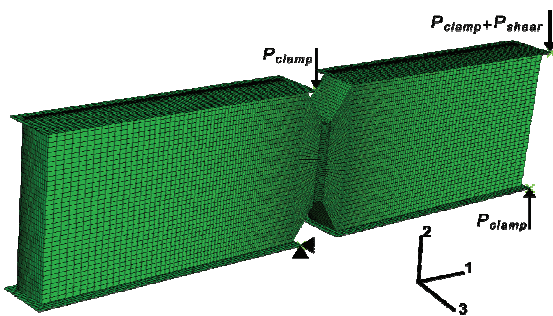


Fig. 3. FE-model for the rhomboidal imperfection with loads, boundary conditions and the coordinate system indicated.

3.1 Isotropic Specimens

For the isotropic specimens, the standard notch opening angle, $2\theta = 110^\circ$, was used, cf. Eq. 1. All

three imperfection types seen in Fig. 2 were studied. Four different imperfection magnitudes were investigated, namely $d = [0.5, 0.1, 0.05, 0.01]$ mm, representing a relatively large to a very small, hardly detectable, imperfection.

3.2 Orthotropic Specimen

For the CFRP specimens with fibers aligned with the test region, the notch opening angle $2\theta = 71^\circ$ was determined from Eqs. 1 and 2 and used here. Since it had been previously found that the type 1 imperfection only has marginal influence in the test region, this type was omitted here. Instead, the focus was on imperfections giving rhomboidal or conical cross sections in the gripping region. Only one magnitude of the parameter d was investigated, viz. $d = 0.21\text{mm}$. This fairly large d was chosen for the experiments, since these were expected to be difficult to perform and evaluate.

4 Numerical Results - Imperfect Specimens

It should here be noted that also the ideal τ_{12} -field is not entirely even: at free the surfaces at both ends of the test region τ_{12} must vanish, and in between it must build up to a rather uniform level which (due to equilibrium reasons) will exceed the nominal (average) shear stress $\bar{\tau}_{12}$. In an ideal situation, there will also be a slight variation through the test region thickness due to 3D effects and stress gradients near the test region.

The two different imperfection types studied, the rhomboidal and the conical cross section, are expected to perturb the nominal (ideal) τ_{12} - profiles in different ways:

The rhomboidal type will cause an anti-symmetrical perturbation along the test region which additionally will be anti-symmetrical through the specimen thickness. There should be no front-to-back difference for the observed mean stress values.

The conical imperfection, on the other hand will give noticeable front-to-back differences, and those will not be even (or even anti symmetrical) through the thickness. Along either face of the test region (or any parallel section within), the stress profiles should remain symmetrical, although that shape may vary through the thickness.

4.1 Isotropic Materials

The numerical results for the chosen isotropic material (aluminum) should be in essence identical among all isotropic materials if specimen thickness is kept constant. Very minute differences among stress profiles may arise for different Poisson's ratios ν , however utterly insignificant for any practical purpose. Additionally, there may arise some (very minor) kinematic non-linearity depending on load level and evolving contact areas. These however vanish if, in the calculations, load levels always are scaled with modulus E .

In Figs. 4ab, normalized stress profiles along the test region for two rhomboidal imperfections are shown at various through-thickness positions. The most pronounced skewness is, of course, observed at the front and back faces, and more for the larger imperfection size $d = 0.1$ mm. The largest difference is near one end of the test region, it is about $\sim 15\%$, and even for a very small imperfection, $d = 0.01$ mm, this difference still remains at $\sim 7\%$. Averaged values are as expected quite similar, however.

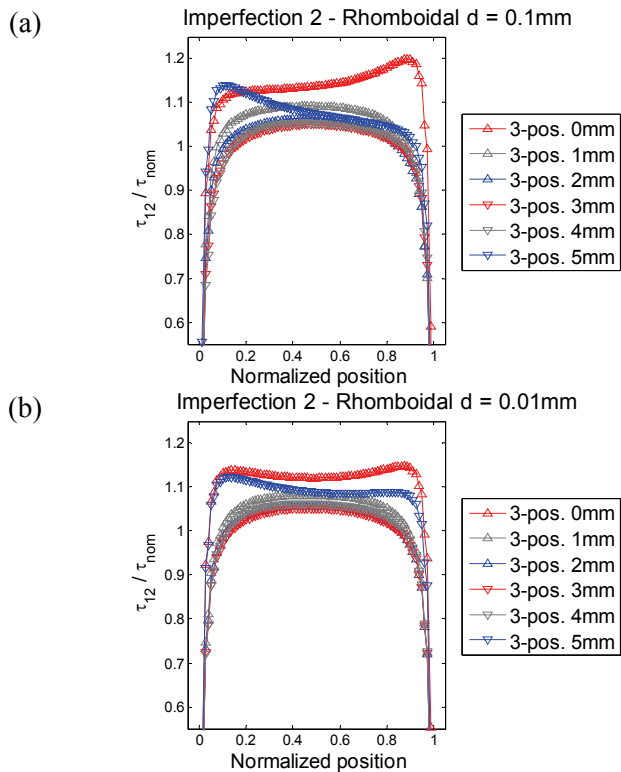


Fig. 4. Normalized test region stress profiles at various through-thickness positions for a rhomboidal imperfection of: a) $d = 0.1$ mm, and b) $d = 0.01$ mm.

In Figs. 5ab, normalized stress profiles along the test region for two conical imperfections, and how they vary through the specimen thickness, are shown. Each of these profiles is symmetrical, but their mean differs vastly from front to back. For the larger imperfections size $d = 0.1$ mm, profile mean stresses on the face with the pointed edges (left side in Fig 2.d), are higher by a factor of 2.65 compared to the opposite face, i.e. higher by 165%. And even for a very minor imperfection of that type ($d = 0.01$ mm), this difference remains at almost 10%. Locally differences may be a bit smaller (in the central part) or even larger (near the ends of the test region). Note also that the lowest mean stress is not found on one of the faces (as opposed to the larger imperfection).

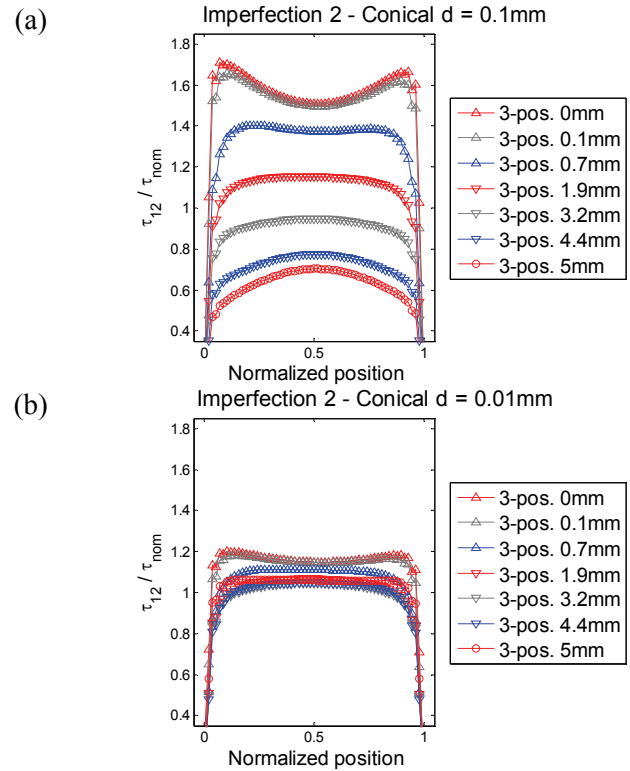


Fig. 5. Normalized test region stress profiles at various through-thickness positions for a conical imperfection of: a) $d = 0.1$ mm, and b) $d = 0.01$ mm.

4.2 Orthotropic Material

For an orthotropic material, it is no longer possible to interpret numerical results more generally. Apart from the possibility of two different material testing directions (which for perfect geometry effectively is handled through rescaling the notch angle, see Eqs. 1 and 2), both the specimen thickness and material elastic properties (and their range of variation) in three directions largely

influence the stress solutions in the composite specimen. Note that for orthotropic elastic materials, there is no coupling between normal- and shear strains, so that shear stress and shear strains profiles can be used interchangeably. They only differ by a factor corresponding to the shear modulus.

Here, the orthotropic material described in Table 1 was used with the stiffer direction along the test region. Resulting stress profiles are shown in Figs. 6 and 7.

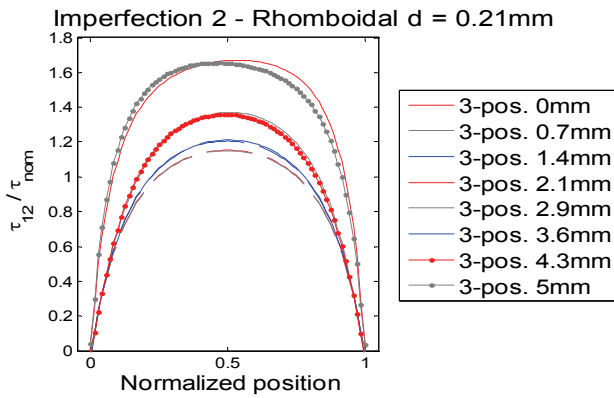


Fig. 6. Normalized test region stress profiles at various through-thickness positions for a orthotropic material with rhomboidal imperfection $d = 0.21$ mm

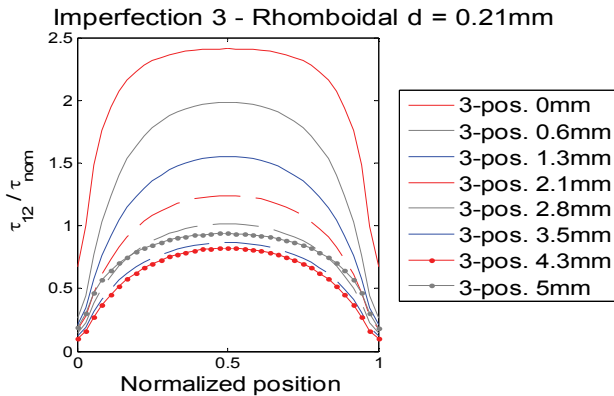


Fig. 7. Normalized test region stress profiles at various through-thickness positions for a orthotropic material with a conical imperfection of $d = 0.21$ mm

Remarkable is that essentially no skewness is observed for the rhomboidal imperfection, although it is a substantial one. Instead, it is noticed that there is a quite large variation in τ_{12} -levels through the thickness. For this material orientation, the highest τ_{12} are always near the middle along the test region (notch root radii influence significantly). However, profile peak values are larger by $\sim 37\%$ at the faces compared to the center of the panel thickness.

On the contrary, for the conical imperfection, the front-to-back difference is immense. Again, peak levels are found in the middle along the test region, but are 2.6 times as high on face with the pointed edges (left side in Fig. 2c), i.e. 160% higher than on the other face. Here, the differences are almost identical to the ones obtained for isotropic materials.

5 Experimental Program

Aluminum specimens were machined for both the rhomboidal and conical imperfection types, and to magnitudes $d = 0.05$ and 0.1 mm. Also CFRP composite specimens with the fibers oriented along the test region were manufactured with both those imperfection types. For the composite material, $d = 0.21$ mm was used. Elastic properties for both materials are given in Table 1. All specimens were individually measured before testing

Shear testing was performed in a servo-hydraulic MTS – testing machine equipped with an Instron control system. An in-house built Iosipescu fixture was used for all experiments. Whole field strain- and displacement fields were optically recorded on both front- and back specimen faces with the DSP-equipment Aramis, by GOM mbH. Both fixture and the optical measuring technique are described in detail elsewhere [6,7].

Experimental testing comprised of photographing the unloaded specimens before clamping, after clamping but still unloaded, followed by manually ramping up the nominal shear load at slow rate and taking photographs at about 20 different load levels up to peak load. Peak loads corresponded to either widespread and substantial plasticity (Al) or specimen failure (CFRP).

6 Experimental Results – Strain Profiles

Strain profiles were calculated from the photographs of loaded and deformed specimens described above. And such profiles are presented here for some different load levels where the highest load is still deemed to be in an overall elastic state of deformation. Further, stress-strain responses are calculated using average strains from each face individually.

6.1 Aluminum Specimens with Imperfections

Fig. 8 shows results for the rhomboidal imperfection, and straight lines are fitted to the central 85% of the profile to guide the eye.

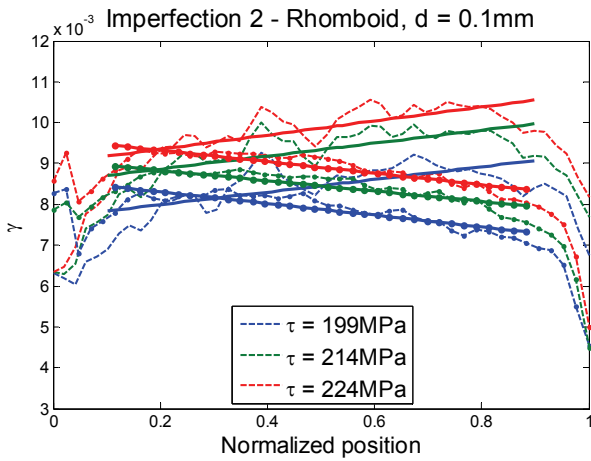


Fig. 8. Front- and back strain profiles at three load levels for an aluminum specimen with rhomboidal imperfection of $d = 0.1$ mm. Dotted lines are front face. Bold straight lines are fitted guide the eye.

In Fig. 9, the constitutive behavior in shear for that aluminum is shown if strain data were taken from only one of the specimen faces. True net shear stress τ_{12} is plotted versus average shear strains γ from profiles such as the ones shown in Fig. 8.

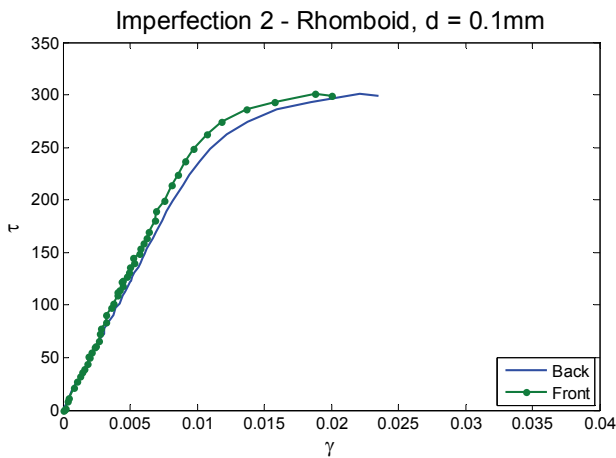


Fig. 9. Apparent stress-strain responses for experiment shown in Fig. 8 if shear strain γ is evaluated only on one specimen face.

As seen, there is a small difference between front and back, but not much larger than one would usually expect in an experiment. Note also that a shear stress of $\tau_{12} = 224$ MPa seems to be not too far outside the elastic regime, if not within.

In Figs 10ab, arising strain profiles for two specimens with conical imperfections are displayed. For both imperfection magnitudes, quite uniform strain profiles are obtained but a large and

systematic front-to-back difference is evident; The difference is about 50% and 26% respectively.

When comparing apparent stress-strain responses based on strains from only one face, the arising difficulties are clearly evident in Figs. 11ab.

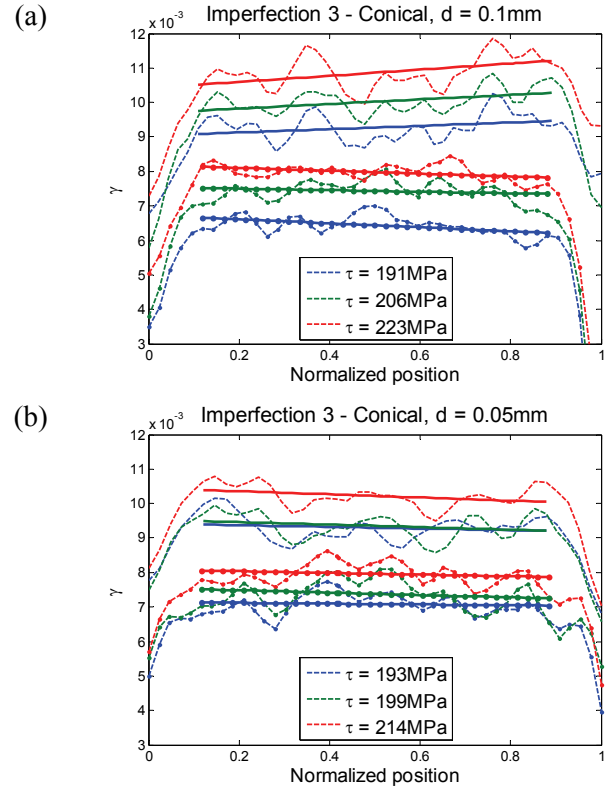


Fig. 10. Front- and back strain profiles at three load levels for an aluminum specimen with rhomboidal imperfection of: a) $d = 0.1$ mm, and b) $d = 0.05$ mm. Dotted lines are front face. Bold straight lines are fitted guide the eye.

6.2 Composite Specimens with Imperfections

Here, similar results are shown as for in the previous section. Among all specimens, the imperfection was $d = 0.21$ mm. Fig. 12 shows front- and back strain profiles for a rhomboidal one.

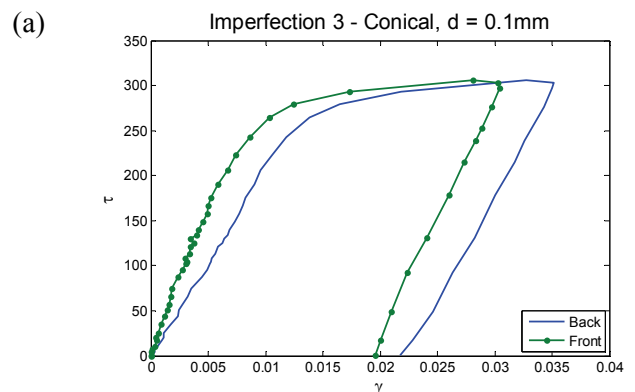


Fig. 11. (continued on next page)

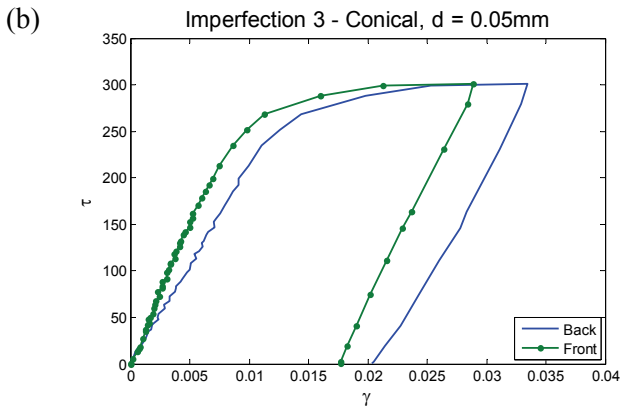


Fig. 11. Apparent stress-strain responses for experiments shown in Figs. 10ab if shear strain γ is evaluated only on one specimen face with a) with $d = 0.1\text{mm}$, and b) with $d = 0.05\text{ mm}$.

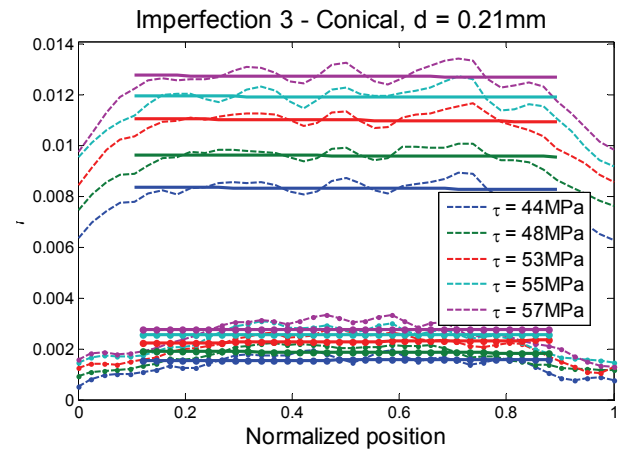


Fig. 13. Front- and back strain profiles at three load levels for a CFRP specimen with conical imperfection. Dotted lines are front face. Bold straight lines are fitted guide the eye.

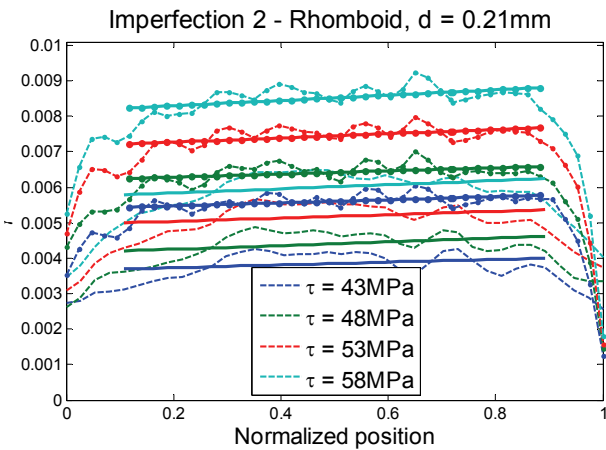


Fig. 12. Front- and back strain profiles at three load levels for a CFRP specimen with rhomboidal imperfection. Dotted lines are front face. Bold straight lines are fitted guide the eye.

And while almost no difference in skewness can be observed (as there was for Al in Fig. 8), there is a notable difference in level (40%) indicating that this experiment must have had other additional sources of error.

For a conical imperfection, back- and front strain profiles are shown in Fig. 13. Again, they are quite uniform, but here extreme differences between the two faces are seen, they seem to differ by a factor in excess of four throughout the test.

Fig. 14, finally shows how extremely misinterpreted constitutive behavior may be if strains were evaluated only on one specimen face if geometrical imperfections are present. And again, this demonstrates that this is even more important for conical imperfections.

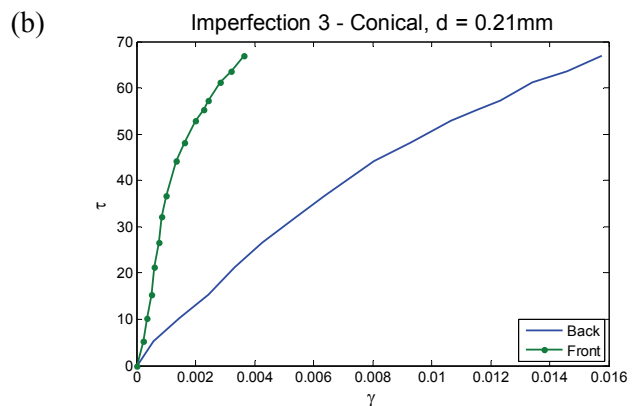
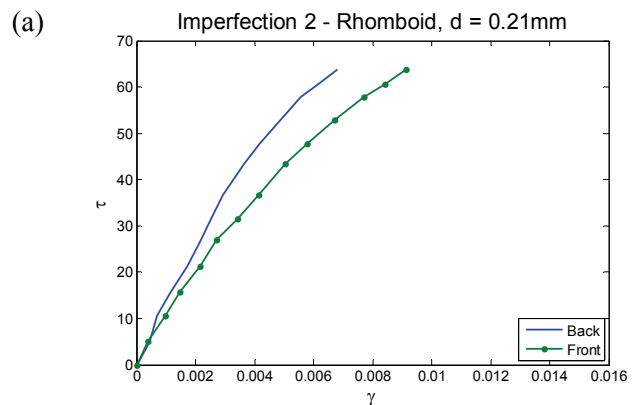


Fig. 14ab. Apparent stress-strain responses for experiments shown in: a) Fig 12, and b) and Fig. 13, if shear strain γ is evaluated on one specimen face

7 Conclusions and Discussion

It has here been shown numerically, and confirmed experimentally, that even minor deviations from nominal specimen geometry may cause significant (not to say enormous) differences in strain profiles between specimen front- and back

side. Even with perfect fixture function, beveled edges in the specimen gripping region cause nominal loads to be introduced eccentrically and thereby severely distort the desired and expected stress- and strain uniformity in the test region.

The main nominal load is introduced at what is referred to ‘the inner loading points’, i.e. at the end of the gripping section nearest to the test region, and on opposing sides on either specimen half (cf. Fig. 1). If these loads additionally are introduced near one of the specimen faces due to beveled gripping surfaces, this results in substantial through-thickness variation of the stress fields. If the two inner loading points are on opposing faces, skewed strain profiles in the test region are the results, and this anti-symmetry shifts direction through the specimen thickness. In this case, measured strain averages on either face will still be representative (within experimental precision and scatter), but at poorer uniformity.

If, instead, the inner loading points both are near the same specimen face, resulting strain profiles will remain symmetrical along the test region, but display large differences in level through the specimen thickness. These differences may very well be in excess of 100%. They depend on relative specimen thickness and also on the details of the near ‘line-like’ contact.

For the more ductile aluminum material, the experimental differences were less than predicted by the numerical analysis for the conical imperfection, while for the rhomboidal one the appearance matched well. Even the concave and conical shapes of the profiles in Fig. 5 agreed with the appearance of (particularly) the measured profiles seen in Fig 10b. Presumably, local plasticity along the contact edges shifts the center of action and lowers the degree of eccentricity compared to the purely elastic numerical calculations. But, although this effect is a favorable one, large differences remain.

When it comes to composites, the orthotropic behavior and the usually quite low through-thickness shear moduli, make such materials less sensitive to the rhomboidal imperfection type. However, in spite of very similar looking profiles on both faces, these measurable strains may not be representative for the average strains throughout the tested volume as they may be much lower in the panel center, as was observed numerically.

The contrary is true with conical imperfections: numerically front-to-back difference is as large as for an isotropic material, but experimentally it proved to be even larger. Again, low through

thickness shear moduli contribute this sensitivity as does panel thickness. Presumably, the effects of, and uncertainties involved with, local deformation and degradation near loading points make composites even more prone to be imperfection sensitive.

This once more emphasizes the inherent difficulties involved in composite shear testing. Admittedly, the imperfections advertently introduced in the CFRP specimens were rather on the large side, but as the Al-specimen and the FE-analyses showed even very small imperfections may distort experimental results to render them nearly useless.

Acknowledgements

The authors are indebted to Mr. B. Möllerberg for manufacturing the fixture, to Mr. B. Dolk for the specimens, Mr. Karim Cherif for shearing them, the Knut and Alice Wallenberg foundation for financing the DSP-equipment, and faculty funding from KTH.

References

- [1] Walrath D.E. and Adams D.F., ‘The Iosipescu shear test as applied to composite materials’. *Experimental Mechanics*, Vol. 12, pp 131–138, 1990
- [2] ‘Standard method for shear properties of composite materials by the v-notched beam method’, ASTM Designation: D 5379/D 5379M-93, 1993
- [3] Neumeister J.M. and Melin L.N. ‘A modified Iosipescu shear test for anisotropic composite panels’, SME: *Proc. ICCM 14*, San Diego, USA, 2003
- [4] Suo Z., Bao G., Fan B. and Wang T.C. ‘Orthotropy rescaling and implications for fracture in composites’. *Int. J. Solids Struct.*, Vol. 28, pp 235–248, 1991
- [5] Pierron F. and Vautrin A., ‘Measurement of the in-plane shear strengths of unidirectional composites with the Iosipescu test’. *Composites Science and Technol.*, Vol. 52, pp. 61-72, 1994
- [6] Melin L.N. and Neumeister J.M. ‘Specimen clamping and performance of the Iosipescu shear test for composite materials’, SME: *Proceedings, ICCM 16*, Kyoto, Japan, 2007
- [7] Neumeister J.M. and Melin L.N. ‘Measuring constitutive shear behavior of orthotropic composites and evaluation of the modified Iosipescu test’, *Composites Structures* Vol. 76, pp 106–115, 2006
- [8] Melin L.N. and Neumeister J.M. ‘The influence of specimen clamping and specimen imperfections on the Iosipescu shear test performance’ Paper C in Licentiate Thesis, KTH – Solid Mechanics no 99, 2006. To be submitted.